Neutralization of 50—230-keV hydrogen ions which have penetrated Al, Au, C, and Cs films

Siegfried Kreussler* and Rudolf Sizmann
Ludwig-Maximilians-Universität München, D-8000 Munich 40, Amalienstrasse 54, Federal Republic of Germany

(Received 6 October 1981)

The fraction of neutral atoms Φ_0 in a beam of hydrogen projectiles (H,D; 50—230 keV) which have penetrated thin targets covering a wide range of atomic numbers and free-electron densities has been measured. Ordinary carbon, gold, and aluminum targets yield identical Φ_0, in agreement with data already in the literature. However, pure gold, aluminum, or cesium evaporated *in situ* on the exit surface of a target foil yield a Φ_0 dependent on the specific material at energies greater than 50 keV/amu. New information on Φ_0 is obtained with solid cesium targets and on its dependence on the target tilt angle towards the beam direction. In the frame of a simple kinetic model Φ_0 is dominated at low energies, 25—50 keV, by charge exchange in the electron blanket at the target surface. At high energies, >250 keV, Φ_0 is determined by the atomic cross sections of charge exchange. Only in the intermediate-energy regime is Φ_0 observed as dependent on the tilt angle of the target surface towards the beam direction.

I. INTRODUCTION

A beam of fast ions penetrating a gas or a foil becomes partially neutralized. In steady state the fraction of neutral particles in the beam Φ_0 is determined by the cross section σ_c of capture of electrons forming the neutral state and the cross section σ_l of loss of electrons from the neutral state[1]:

$$\Phi_0=\sigma_c/(\sigma_l+\sigma_c)\ . \tag{1}$$

Bohr has presented theoretical approximations for σ_c and σ_l,[2] which explain the main characteristics of neutralization in gases.[1] σ_c and σ_l depend on ion energy and atomic numbers Z_1 and Z_2 of ions and target atoms, respectively. Neutralization in solids was discovered in 1922 by Rausch von Traubenberg and Hahn.[3] They observed neutral particles after the passage of canal rays through thin gold foils. Comprehensive experiments with accelerated protons were performed in 1950 by Hall[4] and in 1955 by Phillips.[5] Neutralization in solids was interpreted to be analogous to Bohr's conception of gases: The ions capture and the neutrals loose electrons in single collisions with the atomic nuclei and electrons of the solid. However, Phillips[5] failed in detecting any influence of the target atomic number Z_2 on Φ_0, in contrast to the results obtained in gases. Phillips interpreted this as a contamination effect. A few monolayers of oxides or hydrocarbons at the target surface suffice to establish a neutralization equilibrium characteristic of such contamination layers, thereby producing Φ_0's independent of the substrate material.

To check this assumption, Phillips evaporated *in situ* fresh target material on the exit surface of the foils. Then Φ_0 was found to depend on that target material, indeed. Unfortunately the vacuum conditions were too poor for performing reproducible experiments. At higher energies (>0.5 MeV) the influence of contamination layers on Φ_0 becomes negligible and the interpretation of Φ_0 based on Bohr's atomic cross sections σ_l and σ_c is satisfactory (Chateau *et al.*[6,7]). Recent work[8] confirms that at low energies (1—5 keV) Φ_0 depends critically on the cleanliness of the exit surface. In the medium energy range (25—250 keV) data of Φ_0 with provable clean target surfaces are not available. The present experimental investigation reports on extensive measurements in this energy regime.

The interpretation of neutralization in solid targets is more complex than in gases. In a semiquantitative model proposed by Brandt and Sizmann[9—11] the solid is considered as a stratified system of bulk material covered by a surface blanket of a free-electron gas. A major point is that within the solid the charge of the projectile is shielded by target electrons, especially at low velocities. Then, if bound states of an electron to a

moving proton do not exist within the target the observed neutralization of emerging projectiles occurs during the passage through the exit surface. The conception is that in a collision an (bulk or surface) electron gains a correlation in speed and direction to the projectile. When the projectile leaves the surface and the correlation has not been destroyed by another collision, such a correlated electron can become bound. The quoted model is is based on kinetics, operating with cross sections of electron capture and loss in the bulk and in the electron blanket. Its qualitative success for protons in the energy range above 25 keV is at present its justification. A comprehensive theoretical treatment of neutralization of fast protons has not yet been worked out. The main problem lies in the low-velocity regime, where, e.g., collective electronic properties of the solid target are operative or electrons can be captured by tunnel effect.[8]

We have measured the charge state of a beam of protons or deuterons having penetrated thin foils of Al, Au, C, and Cs, which cover a wide range of nuclear charge Z_2 and electron density.[12] The exit surfaces of these foils are prepared *in situ* by vapor deposition in ultrahigh vacuum. The energy range covered with H^+ and D^+ ions is 50–230 keV/amu, corresponding to velocities of v_0 to $3v_0$, v_0 being Bohr's velocity (cf. Sec. IV A). At constant velocity, the incident angle of the beam towards the normal of the foil is varied. Thereby, the dwell time of the projectile in the vicinity of the surface is changed, which may alter any contribution of surface effects to neutralization.

II. EXPERIMENTAL

H^+ or D^+ are produced in an rf-ion source and are accelerated by a linear accelerator to variable energies between 50 and 230 keV. The ions are then deflected magnetically through an angle of 15° into the target chamber (Fig. 1). The beam is geometrically collimated by two apertures of 0.2-mm diameter with a final beam divergence of 0.02°. Energy straggling in the beam is less than 1 keV; maximum beam current is about 10 nA.

The vacuum in the target chamber is 1×10^{-7} Pa and maintained successively by a turbomolecular pump, an ion getter pump, and a titanium sublimation pump. In the residual gas, hydrocarbons were below the detection level of a mass spectrometer. For degassing, the complete target chamber can be heated up to 450 °C.

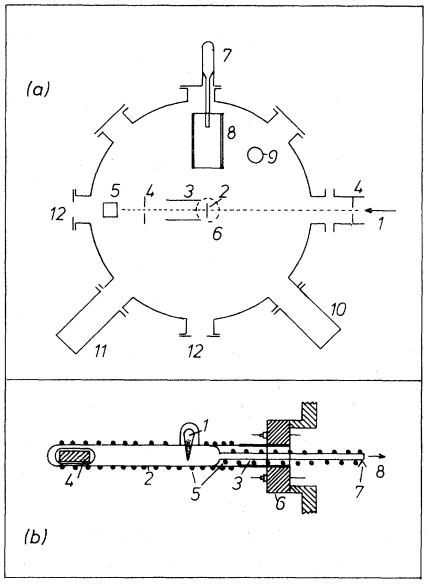

FIG. 1. (a) Target chamber: Beam (1), target foil (2), deflection capacitor (3), beam collimator (4), surface barrier detector (5), electron-gun evaporation source (6), cesium evaporation source (7), glass tube (8), cooling finger filled with liquid nitrogen (9), Auger electron spectrometer (10), mass spectrometer (11), window (12). (b) Cesium evaporation source: Cesium ampoule (1), glass tube (2), capillary (3), piece of iron (4), heating wires (5), Conflat flange (6), thermocouple (7), cesium stream (8).

The polycrystalline targets are self-supporting foils. They are produced by vacuum deposition onto a glass slide, which is covered with a soap film. The evaporated foils are detached in water from the glass substrate and mounted on frames with 15-mm diameter. Typical thicknesses are Al, 25 $\mu g/cm^2$; Au, 100 $\mu g/cm^2$; C, 20 $\mu g/cm^2$. By a vacuum goniometer the foils can be moved in the plane perpendicular to the beam axis; they can be rotated around two axes which are perpendicular to the beam. The axes of the rotation are in the plane of the foil, passing through its center.

Having left the target the projectiles pass through a parallel plate capacitor. The plates are 70-mm long and 20-mm apart. By a voltage of 4.5 kV all the beam ions can be deflected so that they do not reach the silicon surface barrier detector which terminates the optical beam axis about 50-mm downstream the capacitor. The detector is covered with an aperture, so that only projectiles with angular straggling less than 0.2° can be recorded. The detector can be moved by an exter-

nal manipulator in the plane perpendicular to the beam. It is mounted at the end of a tube through which cooling water can flow during thermal degassing of the vacuum chamber. Every projectile, charged or neutral, which enters into the detector produces an electric pulse the height of which is proportional to the energy of the particle. The electric pulses are amplified, analyzed, and recorded by a multichannel analyzer. Because of statistics and noise in the detection and electronic systems even a monoenergetic beam produces a Gaussian energy spectrum with about 12-keV full width at half maximum (FWHM).

The neutralization ratio Φ_0 could be measured as follows: For one minute all particles of the beam are recorded. Then voltage is applied to the capacitor which causes only the neutral particles to reach the detector; they are counted for another minute. The ratio between the number of counts in the two spectra would produce Φ_0. However, short-time beam fluctuations cause this simple method to be rather inexact. Therefore, we need to record both spectra, total and neutral, respectively, almost simultaneously. By a pulse generator logic pulses are produced which sweep the capacitor high voltage at a frequency of about 20 s^{-1}.

Simultaneously, the detector switches to distribute the counts into two distinct memories of the multichannel analyzer. Figure 2 illustrates this working scheme. The time length of the logic pulses can be adjusted to multiples of quartz stabilized 100-ns intervals. At high energies the beam contains about only 5% of neutral atoms. The logic pulses are adjusted in such a way that both parts of the spectrum contain similar count numbers. The high voltage at the deflecting capacitor cannot be switched on or off instantaneously. It takes about 0.5 ms for the voltage to rise up to 4.5 kV and 0.2 ms to return to zero. During these time intervals the separation of ions is not complete. Therefore, the pulse generator produces additional logic pulses for the multichannel analyzer

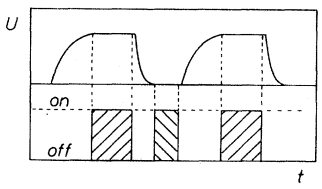

FIG. 2. Deflection capacitor: Time sequence of voltage (U) rise, of open channel for counting the neutrals (///) only, or of total projectiles (\\\).

to restrict the detection time to intervals, where the capacitor voltage is either exactly 0 or 4.5 kV.

For *in situ* preparation of a fresh target surface a target foil is moved into the horizontal plane with its exit surface downwards. About 10 cm beneath the foil there is an electron-gun evaporation source for depositing gold or aluminum onto the foil. 99.995% pure gold and 99.95% pure aluminum are used in the evaporation source. A shutter between the source and the foil catches the first deposits, which in the case of aluminum contains aluminum oxide. Then the shutter is removed. Layers of about 10-nm thickness were deposited within one minute at a pressure of about 5×10^{-7} Pa.

The cesium evaporation source[13,14] is shown in Fig. 1. A glass ampoule with cesium under vacuum is sealed in a wider glass tube. This tube, closed at one end, is fixed with a conflat flange to the target chamber. A capillary connecting the glass tube and the vacuum chamber allows us to evacuate the tube. In the tube there is a piece of iron sealed into glass, which by a magnet can be moved towards the cesium ampoule for breaking it. The tube and the capillary are resistance heated up to 170 and 200 °C, respectively. The cesium evaporates and a stream of cesium vapor leaves the capillary causing a cesium deposition onto a gold foil. For producing thick and uniform layers the foil has to be cooled. Therefore, the target manipulator is connected by a flexible copper cable to a cooling finger filled with liquid nitrogen. By this the target foil reaches temperatures as low as −70 °C. A cesium layer of about 10 nm is evaporated in 30 minutes.

Foil thicknesses can be calculated from energy loss of penetrating ions. An energy loss of 10 keV can be measured with an accuracy of about 1 keV. The diameter of the foil is 15 mm, of the beam 0.2 mm. This allows thickness measurements in various spots of the foil. Within the experimental uncertainty the foils were found to be uniform. By evaporation of fresh layers of gold, aluminum, or cesium the foil thicknesses remained uniform. Some of the foils used in the experiments were analyzed by a scanning electron microscope. Up to a magnification of 15 000 neither the target foils nor the evaporated layers showed any surface structure. The cleanliness of evaporated gold layers was checked by Auger electron spectroscopy of the surfaces. Gold foils which had been handled in air showed a carbon surface contamination. At the freshly evaporated surfaces carbon or other

contaminations were not detectable.

In the experimental procedure at first a spectrum of the direct beam is recorded. Then the target foil is moved into the beam in a normal incidence position and the oscillating high voltage is applied to the deflecting capacitor. In channel numbers 0 to 256 of the analyzer only the neutral atoms are counted; the spectrum of all particles is accumulated in channels 256 to 512. Then the foil is tilted 60° towards the beam direction and the measurements are repeated. By changing the primary energy of the proton beam in steps of 10 keV such measurements were performed in the range of 50 to 230 keV. For even lower projectile velocities deuterons instead of protons were used.

The maximum of every recorded spectrum is calculated by a parabola approximation in the peak region. In this way the peak position can be found with an accuracy ± 0.3 channels, which corresponds to the statistical uncertainty of the relevant accumulated counts. Such maximum positions of the primary beam spectra are plotted versus the calibrated instrument readings of the accelerating voltage. By a least-squares fit a linear relation is found, which allows the absolute particle energy to be reproducibly adjustable within ± 5 keV.

In the spectrum of the neutrals the counts in the channel with the maximum and in three channels left and right of this maximum are summed (taking three or more channels is not critical). Analogously, the counts around the maximum of the spectrum of total projectiles are summed. The ratio of the two sums corrected for the respective counting times corresponds to Φ_0. The energies of the two corresponding maxima positions are almost identical and any correction is inessential. By an analytical calculation with taking into account the finite resolution of the detector it can be shown that the systematical error of the present evaluation procedure is less than the about 1% statistical error of the measurements.

III. RESULTS

In Figs. 3 and 4 the experimental results (Φ_0 in percent) are plotted versus $(1+v^2)$, where v, the exit velocity of the projectile ions H^+ and D^+ is

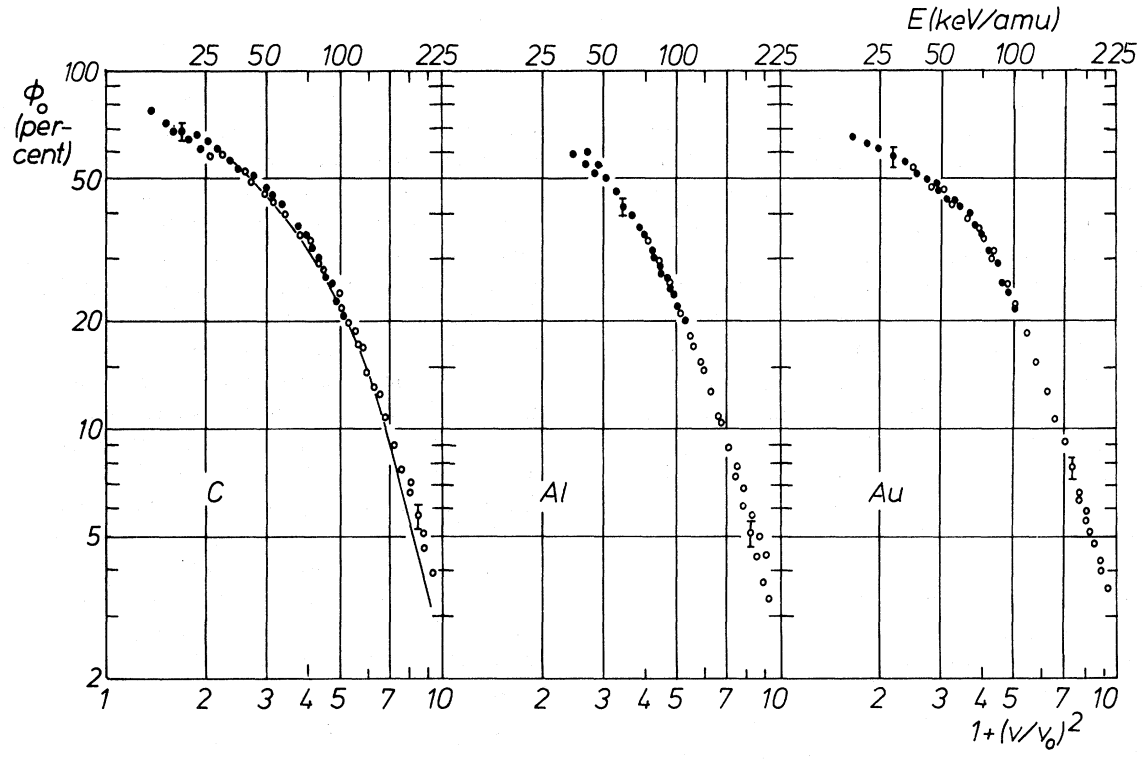

FIG. 3. Fraction of neutral projectiles (Φ_0 in percent) in the beam (● deuterons, ○ hydrogen ions) after penetrating contaminated foils vs velocity $(1+v^2)$ or energy/amu. The target foils were carbon (~ 18 μg/cm^2), aluminum (~ 20 μg/cm^2), and gold ($\sim 90-110$ μg/cm^2).

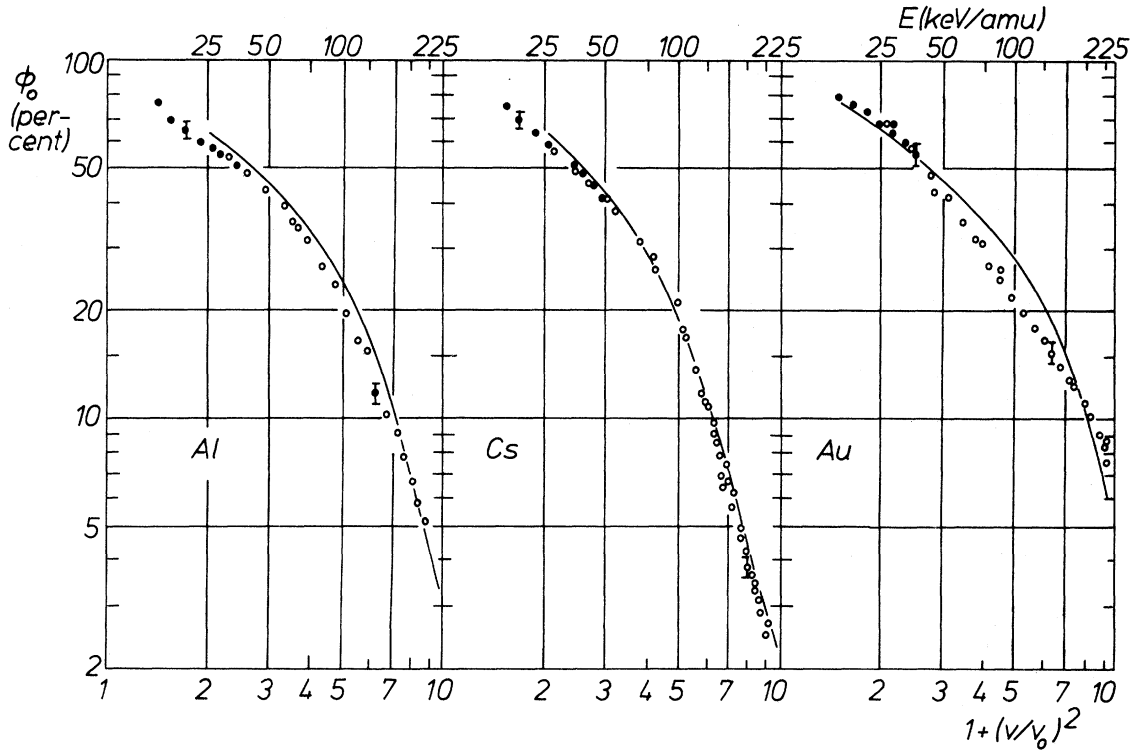

FIG. 4. Fraction of neutral projectiles (Φ_0 in percent) in the beam (● deuterons, ○ hydrogen ions) after penetrating foils with *in situ* evaporated layers of Al, Au, or Cs on the exit surface.

given in units of Bohr's velocity v_0. The direction of incidence is normal to the target foil. Φ_0 is primarily a function of velocity, not of energy of the projectiles. Deuterons were used for extending the scale towards smaller velocities. In Fig. 3 results with carbon, gold, and aluminum are shown. These foils were not produced *in situ* and, therefore, they are inevitably contaminated. In Fig. 4 results with *in situ* prepared surfaces are shown. The evaporated layer thickness is 20 to 50 nm which is, at the low velocities used, sufficient to establish an equilibrium characteristic of pure bulk material. The *in situ* evaporated gold layers did not contaminate in 24 h in a vacuum of 1×10^{-7} Pa. However, if such a foil was stored in air for 24 h and then mounted again in the target chamber, the measured Φ_0 were the same as found with a contaminated foil.

With an additional evaporation of about 10 nm of fresh gold the characteristics of clean gold are found again. A change of Φ_0 by any contamination which may build up during the first minutes after evaporation of gold was not detectable. Therefore, we conclude that the gold surfaces were clean and remained so for about 24 h. After evaporation of fresh aluminum on an aluminum target foil repeated measurements showed no indication of a progressive contamination during hours of experiments. The *in situ* evaporated cesium layers changed in vacuum within a few hours, then producing Φ_0 values like a carbon foil. After evaporation of a fresh cesium layer, the initial results are found again. All points in Figs. 3 and 4 have been measured with target foils perpendicular to the beam. For the same energies measurements with the foil 60° inclined to the beam have been performed. The observed differences are small and almost comparable to the experimental fluctuations. Therefore, we used a particular way of presenting the data. Having so many Φ_0 at 0° inclination and various proton velocities v available we first determined a smooth curve. It is known[9–11] that in a plot of $\ln\Phi_0$ vs $\chi=\ln(1+0.7v^2)$ a slightly curved line results. A parabola was calculated by a least-squares fit:

$$\ln\overline{\Phi}_0(v,0°)=a\chi^2+b\chi+c\ . \tag{2}$$

In Table I the coefficients a,b,c are listed.

From this analytical function $\overline{\Phi}_0$ (0°) can be calculated in good approximation for any exit velocity

in the measured interval. For every experimental point $\Phi_0(v,60°)$ measured with a 60° inclined foil the percental difference φ_0

$$\varphi_0(v)=\frac{[\bar{\Phi}_0(v,0°)-\Phi_0(v,60°)]100}{\bar{\Phi}_0(v,0°)} \tag{3}$$

is calculated. φ_0 is plotted versus v^2 in Fig. 5. It will be discussed in Sec. IV B. In any tilt experiment, the exit angle of the projectiles towards the local microscopic surface normal is important. There are indications that structural roughness of the exit surface diminishes the extent of such effects.

TABLE I. By a least-squares fit parabolas are calculated through all experimental points with 0° inclination between beam axis and foil normal: $\ln\bar{\Phi}_0(v,0°)=a\chi^2+b\chi+c$, $\chi=\ln(1+0.7v^2)$. v: exit velocity of the projectile in units of Bohr's velocity $v_0=2.19\times10^6$ ms^{-1}.

Target	a	b	c	Energy regime (keV/amu)
C	−1.07	0.69	4.08	50–230
Al	−0.90	0.35	4.17	50–230
Cs	−0.28	−0.62	4.51	30–84
Cs	−0.99	−0.28	5.14	84–230
Au	−0.23	−0.89	4.70	50–230

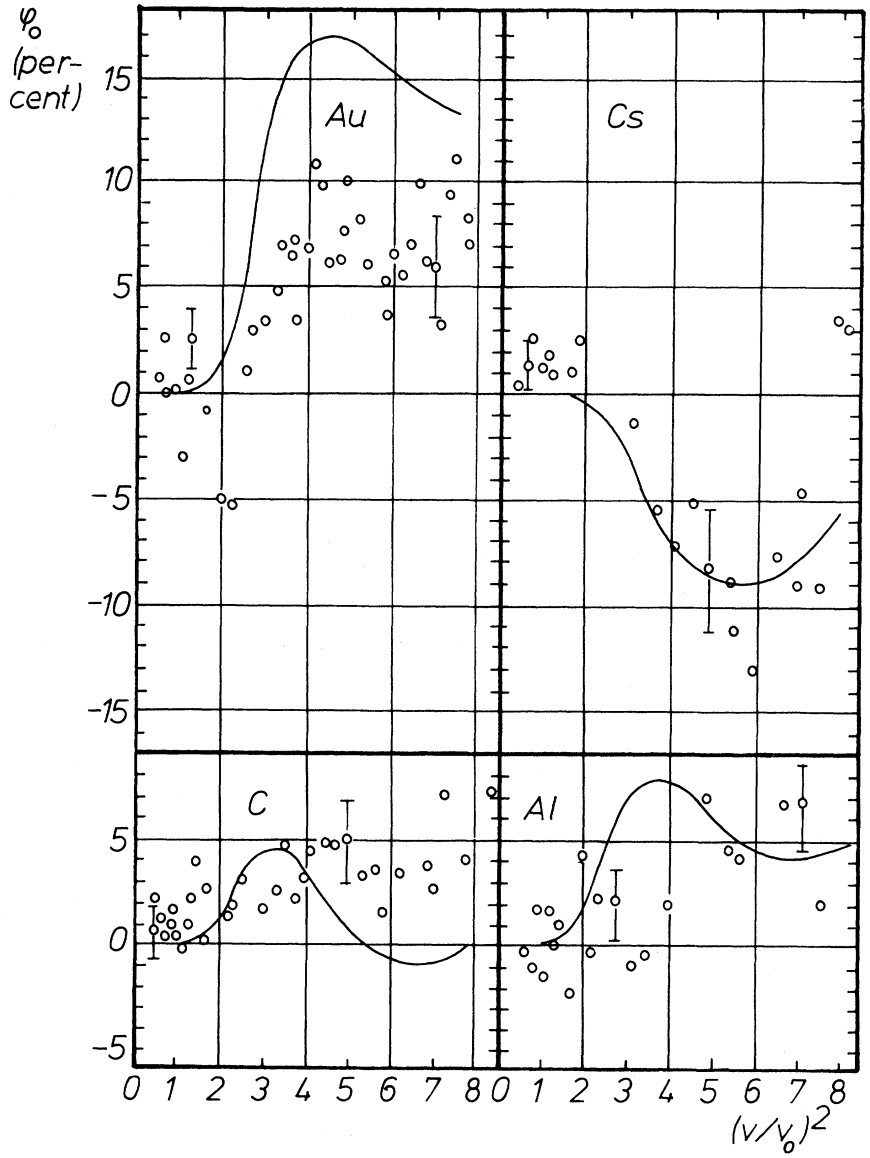

FIG. 5. Percental relative difference of Φ_0 for different tilt angles (φ_0) vs exit velocity. The carbon foil was contaminated; gold, aluminum, and cesium were evaporated *in situ*.

IV. DISCUSSION

In the Introduction the present unsatisfactory status of theoretical considerations to the neutralization of light ions has been addressed. Thus we are left with a kinetic model for calculating Φ_0,[11] which is mainly a guide line for discussing the experimental results.

A. Kinetic model of neutralization

We consider the solid to be a dense atomic gas. Then in steady state the equilibrium value of Φ_0 found after penetration of the (sufficiently thick) target is

$$\Phi_{0_A}=\sigma_{cA}/(\sigma_{cA}+\sigma_{lA}) . \tag{4}$$

Bohr[2] has given approximations for the atomic cross sections of electron capture σ_{cA} and of electron loss σ_{lA} for protons in the relevant energy regime $1\leq v\leq 3$:

$$\sigma_{cA}=4\pi a_0^2 Z_2^{1/3} v^{-6} , \tag{5}$$

$$\sigma_{lA}=\pi a_0^2 , \tag{6}$$

where

$$a_0=\hbar^2/me^2=0.529\times 10^{-10}\ \text{m} . \tag{7}$$

v is in units of

$$v_0=e^2/\hbar=2.19\times 10^6\ \text{ms}^{-1} . \tag{8}$$

The factor 4π in Eq. (5) agrees well with electron-capture measurements in gaseous cesium.[15] Experimental data on solid C, Al, Au (Refs. 4–7, 16–19) and on gaseous He, Ne, O_2, N_2 (Ref. 1) require a factor of 12π in Eq. (5). At the target exit surface there is a blanket of electrons with electron density $\rho(x)$ decreasing with distance x from the surface. The projectile beam interacts with the blanket electrons, changing its initial neutralization Φ_0 to the finally observed Φ_{0_A}.

$$\frac{d\Phi_0(x)}{dx}=\rho(x)\sigma_{cV}\Phi_1(x) - a\rho(x)\sigma_{lV}\Phi_0(x) . \tag{9}$$

$\Phi_1(x)$ is the fraction of ions in the beam $\Phi_1=1-\Phi_0$.

The appropriate cross sections for capture σ_{cV} and loss σ_{lV} in an electron gas are[2]:

$$\sigma_{cV}=4\pi a_0^2 v^{-4}\exp[-b(v-1)^2] , \tag{10}$$

$$\sigma_{lV}=4\pi a_0^2 v^{-2} . \tag{11}$$

The Gaussian factor in (10) is a plausible adjustment of Bohr's capture cross section to guarantee σ_{cV} to decrease steeply at high velocities as required by quantum-mechanical calculations of the capture process.[20] b is an empirical parameter which we adjusted to 0.5.

A moving charged projectile attracts electrons. Therefore, $\rho(x)$ in (9) is not identical with the unperturbed electron density $\rho_0(x)$, but has to be corrected by an electron enhancement factor h which is dependent on the velocity v of the projectile and the local initial density $\rho_0(x)$. A moving neutral hydrogen atom will also enhance its neighboring electron density but to a lesser extent, which is taken into account by the factor a in (9); a is empirically close to 0.55, which is a plausible value. The undisturbed electron density at the surface declines exponentially with width $a_s\sim(r_s)^{1/2}$, where r_s is the Wigner-Seitz radius in an electron gas of density ρ_0:

$$\rho_0(x)=(\rho_0/2)\exp(-x/a_s) . \tag{12}$$

Almbladh *et al.*[21] calculated the enhancement quantum mechanically with the result that the enhanced electron density is almost independent of the undisturbed electron density $\rho_0(x)$ and approximately $\rho^*=0.5a_0^{-3}$. Such a density is comparable to the mean electron density in a hydrogen atom. Therefore, we used an enhancement factor h,

$$\rho(x)=\rho_0(x)h=\rho_0(x)\{1+\rho^*/[\rho_0(x)v]\} , \tag{13}$$

where we followed the arguments of Brandt[10] to its velocity dependence. Thus, the effective electron density $\rho(x)$ is at small velocities almost independent of the material. However, in (13) the blanket density $\rho(x)$ does not vanish even at $x\to\infty$. That is not correct. We must modify $\rho(x)$ in such a way that the effective electron density has dropped to zero at a plausible distance $x=c$ which is of order of the diameter of a neutral hydrogen atom $c=2$. The simplest relations to fulfill this are

$$\rho(x)=(\rho_0/2)\exp(-x/a_s)+\rho^*/v , \quad 0\leq x\leq c \tag{14}$$

$$\rho(x)=0, \quad x>c . \tag{15}$$

The solution for Φ_0 is according to (9) with the initial condition of steady state attained in the bulk of the target material,

$$\Phi_0 = \Phi_{0_A} \exp(-S) + \Phi_{0_S}[1-\exp(-S)] , \tag{16}$$

where Φ_{0_A} is given by (4) and

$$\Phi_{0_S} = \sigma_{cV}/(\sigma_{cV}+\sigma_{lV}) \tag{17}$$

is the steady state neutralization in the blanket electron gas, with parameter

$$S = (\sigma_{cV}+a\sigma_{lV})(c\rho^*/(v\cos\alpha) + \{1-\exp[-c/(a_s\cos\alpha)]\}a_s\rho_0/2) . \tag{18}$$

Here, $\exp(-S)$ appears as weighting function between the contribution of steady state atomic bulk neutralization Φ_{0_A} and electronic surface neutralization Φ_{0_S} in the observed neutralization Φ_0. If the foil is tilted relative to the beam axis by an angle α the effective path length c of the projectile in the electronic blanket is increased to $c/\cos\alpha$.

B. Comparison with experimental data

With (16)–(18) we can calculate Φ_0 for Al, Au, and C, and according to (3) the variation φ_0 of Φ_0 with tilting of the foil. Electron densities ρ_0 for these materials are taken from tabulations of Isaacson.[22] We have chosen such different targets in order to have a broad spectrum of atomic numbers Z_2, and, last but not least, of free-electron densities $\rho_0 = 3/(4\pi r_s^3 a_0^3)$. In Table II the relevant values are listed. The various cross sections are calculated using Bohr's approximate relations.[5,6,10,11] In the case of cesium charge-exchange measurements in cesium gas are available.[15] We have used these data for deriving an experimental atomic neutralization Φ_{0_A} which we used in (16) to calculate Φ_0 and φ_0. The deviation between the experimental Φ_{0_A} and a "theoretical" Φ_{0_A} based on Bohr's atomic cross sections amounts for cesium to within 25% in the velocity regime $2 \le v \le 3$.

The calculated Φ_0 and φ_0 are shown as solid lines in the data plots in Figs. 3–5. The adjustable parameters used in the present calculations are $a = 0.55$, see Eq. (9); $b = 0.5$, see Eq. (10); $c = 2$, see Eq. (14). Their numerical values are plausible in order of magnitude.

TABLE II. Target metal properties.

Target	Atomic number Z_2	Free-electron density (a_0^3)	Electron Wigner-Seitz-radius r_s (a_0)
C	6	5.8×10^{-2}	1.6
Al	13	2.5×10^{-2}	2.12
Cs	55	1.2×10^{-3}	5.88
Au	79	7.2×10^{-2}	1.49

The calculated Φ_0 and the experimental data points of Al, C, and Cs agree well. With Au a systematic deviation is seen in Fig. 4, particularly at the higher velocities, where the atomic Φ_{0_A} is dominant; here Bohr's cross sections (5) and (6) are possibly unsatisfactory approximations.

The calculated φ_0 resemble the experimental φ_0 in the main characteristics. φ_0 is related to the derivative $d\ln\Phi_0/d\alpha$ and we cannot expect the present simple kinetic model for Φ_0 to agree well even in derivatives of Φ_0.

At small velocities, $1 \le v \le 1.7$, there is no tilt effect, indicating that the observed Φ_0 is dominated by the steady state value Φ_{0_S} in the electron blanket. At velocities greater than $v = 1.7$ the tilt effect attains a φ_0 of order of 5% with Al and C, -10% with Cs, and $+8\%$ with Au. A significance of the maximum and minimum values of the calculated φ_0 cannot be considered profound.

C. Comparison of present results with other experimental data

The present experiments in the range $1 \le v \le 3$ with contaminated foils yield identical Φ_0 independent of the target material C, Al, Au; see Fig. 3. The results agree with literature data: C, Refs. 6, 7, 16, and 18; Al, Refs. 4 and 5; Au, Refs. 4–7, and 19.

Gold evaporated *in situ* on the target foil enhances Φ_0 distinctly at proton energies greater than 150 keV. The few measurements of Phillips with *in situ* evaporated gold agree with these results. Phillips also tried to produce clean aluminum surfaces, but the vacuum conditions were less favorable than in the present experiments. This is probably the reason that for aluminum, Phillips's results do not coincide with our measurements. With cesium foils there are no comparable results available, except for Φ_0 in gaseous Cs,[15] as already

mentioned in Sec. IV A. Variation of Φ_0 with the exit angle of the projectile towards the target foil normal has been studied by Phillips; reproducible results were not obtained. Other investigations of such tilt effects on Φ_0 have so far not come to notice.

D. Conclusion and summary

The experimental results on neutralization of moving protons discussed in the frame of a kinetic model of neutralization lead to the following conclusions.

(i) At low energies, 25 to 50 keV/amu, Φ_0 is determined by the steady state value Φ_{0_S} of a hydrogen projectile penetrating the electron blanket on the exit surface of the target; see Eq. (17). The enhancement produces an almost constant electron density around the moving projectile, even if the unperturbed electron density varies widely with target material. The consequence is that Φ_0 appears to be independent of the target material used. A tilting of the foil increases geometrically the path length in the electron blanket but steady state is already attained with zero tilt angle. This explains the observation that at low energies tilting has no influence on Φ_0.

(ii) At energies greater than 250 keV/amu the electron capture cross section and also the electron loss cross section in the electron blanket have become so small that the short path length in such a surface does not any more affect neutralization. Then the observed Φ_0 is identical with the steady state value Φ_{0_A} determined by the bulk of the target; see Eq. (4). The atomic cross sections in Φ_{0_A} depend strongly on target material. In the present approximation the solid target is considered equivalent to a gas target. With pure surfaces there can be no tilt effect in this energy regime, in agreement with the experiments. However, even thin contamination layers at the exit surface of the target may still influence the atomic neutralization and therefore the observed Φ_0. A tilt effect on Φ_0 is then attributed to such a contamination layer.[17]

(iii) At even higher energies, >0.5 MeV/amu, the atomic cross sections have decreased further. The path length to obtain steady state Φ_{0_A} has become long enough so that thin contamination layers at the surface have lost their influence on the observed Φ_0. In this case the material dependence of $\Phi_0=\Phi_{0_A}$ can be reliably measured even without clean surfaces.[6,7] There is no tilt effect left.

(iv) In the intermediate energy regime of 75–250 keV/amu the initial steady state Φ_{0_A} determined by the target material is modified during passage through the surface electron blanket. A tilting of the foil increases the path length in the electron blanket, giving more weight to it; the observed Φ_0 approaches Φ_{0_S}. The intermediate energy regime is, therefore, eminently suited for checking experimental reproducibility and theoretical insight in the neutralization of protons having penetrated solid targets.

ACKNOWLEDGMENTS

This investigation was sponsored by the Bundesministerium für Forschung und Technologie. We are grateful to Dr. Werner Brandt for discussions. Particularly, one of us (R.S.) wishes to thank Dr. Brandt for the extensive cooperation in the present subject.

---

*Present address: Siemens Ag, D-8000 Munich 40, Frankfurter Ring 152.

[1]S. K. Allison, Rev. Mod. Phys. 30, 1137 (1958).

[2]N. Bohr, K. Dan. Vidensk. Selsk. Matt. Fys Medd. 18, (8) (1948).

[3]H. Rausch von Traubenberg and J. Hahn, Z. Phys. 9, 356 (1922).

[4]Th. Hall, Phys. Rev. 79, 504 (1950).

[5]J. A. Phillips, Phys. Rev. 97, 404 (1955).

[6]A. Chateau-Thierry, A. Gladieux, and B. Delauny, Nucl. Instrum. Methods 132, 553 (1976).

[7]A. Chateau-Thierry and A. Gladieux, in *Atomic Collisions in Solids* (Plenum, New York, 1975), p. 307.

[8]W. Eckstein and F. E. P. Matschke, Phys. Rev. B 14, 3231 (1976).

[9]W. Brandt and R. Sizmann, cf. Ref. 7, p. 305.

[10]W. Brandt, cf. Ref. 7, p. 271.

[11]W. Brandt and R. Sizmann, Phys. Lett. 37A, 115 (1971).

[12]We are grateful to Dr. H. J. Maier and his co-workers

for the foil preparation.
[13]H. Jakusch, thesis, University of Karlsruhe, 1973 (unpublished).
[14]S. Kreussler, thesis, University of Munich, 1980 (unpublished).
[15]R. J. Girnius, C. J. Anderson, and C. W. Anderson, Phys. Rev. A 16, 2225 (1977).
[16]B. T. Meggitt, K. G. Harrison, and M. W. Lucas, J. Phys. B 6, L362 (1973).
[17]S. Kreussler, Diploma thesis, University of Munich, 1974 (unpublished).
[18]K. H. Berkner, I. Bornstein, R. V. Pyle, and J. W. Stearns, Phys. Rev. A 6, 278 (1972).
[19]T. M. Buck, L. C. Feldman, and G. H. Wheatley, Surf. Sci. 35, 345 (1973).
[20]H. C. Brinkman and H. A. Kramers, Proc. Acad. Sci. Amsterdam, 33, 973 (1930).
[21]C. O. Almbladh, U. v. Barth, Z. D. Popovic, and M. J. Stott, Phys. Rev. B 14, 2250 (1976).
[22]D. Isaacson, *Compilation of r_s Values,* New York University, Document No. 02698 (National Auxiliary Publication Service, New York, 1975).